Assessment of relative- and absolute-calibration lidar elastic inversion algorithms for high-resolution particle-aerosol optical properties retrieval

Villalba-Torres, S.[a,b], Fernández-Carvelo, S.[a,b], del Águila, A.[a,b], Canella-Ortiz, A.[a,b], Muñiz-Rosado, J.[a,b], Navas-Guzmán, F.[a,b], Ortiz-Amezcua, P.[c], Guerrero-Rascado, J.L.[a,b], Valenzuela-Gutiérrez, A.[a,b], Alados-Arboledas, L.[a,b] and Bravo-Aranda, J.A.[a,b]

[a] Andalusian Institute for Earth System Research, University of Granada, Granada, 18006, Spain

[b] Department of Applied Physics, University of Granada, Granada, 18071, Spain

[c] Department of Physics, University Carlos III of Madrid, Madrid, Spain

Keywords: High spatiotemporal resolution, lidar calibration, inversion algorithm

Presenting author email: samuelvillalba@ugr.es

Abstract: This work compares the performance of the relative-calibration Klett-Fernald inversion algorithm against absolute-calibration inversion approaches to determine high-resolution particle-aerosol optical properties from elastic lidar measurements. Algorithms are evaluated during a Saharan dust intrusion event observed with the multiwavelength Raman-polarization lidar ALHAMBRA at AGORA observatory in Granada, Spain. The results demonstrate better adaptability of absolute-calibration methods for tracking and classifying aerosol layers and clouds, as they present lower temporal variance than relative-calibration algorithm.

1. Introduction

Lidars are essential for continuous atmospheric aerosol monitoring [1,2]. Different strategies exist to retrieve particle optical properties from elastic lidar signals, the most common being the Klett-Fernald algorithm [3]. This method requires a relative calibration at a reference height $\left(z_{ref}\right)$ where the particle backscatter coefficient $\left(\beta_p\right)$ is known—typically in a free-aerosol height where $\beta_p\left(z_{ref}\right) = 0\,Mm^{-1}sr^{-1}$. However, the low signal-to-noise ratio (SNR) at these altitudes usually necessitates temporal averaging of 15–30 minutes to retrieve an accurate backscatter profile. Such averaging limits the ability to track rapid atmospheric processes, including aerosol mixing dynamics and the evolution of short-lived cloud or aerosol layers. In this work, we compare the well-established relative-calibration algorithm (Klett-Fernald) against three absolute-calibration approaches: the iterative algorithm presented by [4], the quasi-backscatter approach proposed by [5], and the forward iterative method described by [6]. These four methods are assessed to evaluate their performance in determining aerosol optical properties at the instrument's native 1-minute resolution.

2. Instrumentation

The experimental results presented in this study were obtained using the Dual-LMRD lidar system (Raymetrics S.A., Greece), named ALHAMBRA, which is currently operational at the urban station of the University of Granada (UGR), Granada, Spain (37.164° N, 3.60° W), as part of the AGORA (Andalusian Global ObseRvatory of the Atmosphere) initiative. AGORA consists of several sites allowing the coverage of different atmospheric backgrounds [2]. The system is also included in the European Aerosol Research Lidar Network (EARLINET) and the ACTRIS (Aerosol, Clouds and Trace Gases Research Infrastructure) [7].

ALHAMBRA consists of two complementary subsystems: a near- and a far-range modules. The near-range subsystem, operating in a biaxial configuration, employs a lower-energy laser (80 mJ per pulse) and features a relatively low full-overlap height (z_{ov}) of approximately 200 m agl. Nevertheless, measurements obtained with this subsystem exhibit a good SNR up to altitudes of about 12 km agl. The near-range subsystem includes elastic detection at 1064, 532, and 355 nm, N_2 vibrational Raman detection at 532 and 355 nm, and depolarization capabilities at 532 and 355 nm. Measurements from this subsystem were used to minimize the uncertainty introduced by the incomplete overlap region in the absolute-calibration inversion algorithms.

3. Methodology

3.1. Elastic inversion algorithms

The range-corrected signal (RCS) for a certain range z at the wavelength λ can be described for each channel by the lidar equation:

$$RCS(z,\lambda) = K(\lambda)\, O(z,\lambda)\, \beta(z,\lambda)\, T^2(z,\lambda) \quad (1)$$

where $K(\lambda)$ is the lidar calibration factor, $O(z)$ is the overlap function, $\beta(z,\lambda)$ is the total backscatter coefficient, and $T(z,\lambda)$ is the atmospheric transmittance, respectively.

The particle backscatter coefficient β_p is widely retrieved using the Klett-Fernald algorithm [3]. This method relies on relative-calibration at a reference height, requiring specific atmospheric conditions (e.g., absence of low-level clouds) and a high enough SNR. The latter is usually achieved by spatial, temporal or spatiotemporal averaging of the RCS, decreasing the resolution. In contrast, a set of absolute-calibration inversion algorithms [4–6] have shown promising results at higher temporal resolution, although a prior determination of $K(\lambda)$ is required. Table 1 shows the absolute- and relative-calibration algorithms used in this study, detailed as follows: the iterative backscatter algorithm is based on the comparison between the lidar signal and the signal expected in a purely molecular atmosphere [4]. The influence of particle aerosols on atmospheric optical properties is gradually introduced into the inversion. Initially, the particle extinction coefficient is assumed to be zero ($\alpha_p = 0\ Mm^{-1}$), and the algorithm is then iterated up to a maximum number of iterations or until the differences between β_p in two consecutive iterations become negligible. At each iteration, β_p is updated using a particle transmittance T_p computed from the particle extinction coefficient obtained in the previous iteration, where $\alpha_p = LR\, \beta_p$, where LR is the lidar ratio. The quasi-backscatter approach is equivalent to the first iteration of the iterative algorithm [5]. The forward iterative algorithm extends the procedure established by [4] by repeating the iterative process at each altitude, starting from an initial height z_0, and progressively accumulating the particle extinction to determine the backscatter at the next level [6]. The primary limitation is that these algorithms fail to converge if $\beta^{att} < \beta_m^{att}$, i.e., at the ultraviolet wavelength (355 nm).

Table 1. Input and limitations of elastic lidar inversion algorithms

Algor.	Input	Restrictions
Klett-Fernald	RCS, β_m, α_m, LR, z_{ref}	Temp. av. to increase SNR at z_{ref}
Iterative	RCS, β_m, α_m, LR, z_{ov}, K	$\frac{RCS(z)}{K} \geq \beta_m^{att}(z)$
Quasi	RCS, β_m, α_m, LR, z_{ov}, K	$\frac{RCS(z)}{K} \geq \beta_m^{att}(z)$
Forward	RCS, β_m, α_m, LR, z_0, K	$\frac{RCS(z_0)}{K} \geq \beta_m^{att}(z_0)$

3.2. High-resolution products

The methodology follows a structured workflow divided into two main stages (Fig. 1):

1. **Calibration Factor Retrieval:** A representative value for K was retrieved using methods like those proposed by [5]. A 3-month lidar dataset was processed, selecting nighttime periods characterized by stable atmospheric dynamics and the absence of low-level clouds. Determining K requires β_p profiles, so the Klett-Fernald algorithm was applied at a 15-minute resolution using an automated z_{ref} selection [8] and a fixed LR of with a representative value of 55 sr [5]. The resulting database demonstrated high stability, with variation coefficients of only 8.2% at 532 nm and 7.3% at 1064 nm. This calibration factor allowed us to obtain the attenuated backscatter coefficient β_{att} as a preliminary step for the absolute-calibration inversion algorithms.

2. **High-Resolution Inversion and Performance Evaluation:** The three absolute-calibration algorithms and the relative-calibration Klett-Fernald algorithm were applied to lidar measurements of a Saharan dust intrusion over Granada on 24–25 April 2025 at the instrument's native 1-minute resolution. The aerosol optical depth (AOD) derived from each algorithm was compared against AERONET (AErosol RObotic NETwork) sun-photometer data (between 10:00 and 15:00 UTC on 24

April) to estimate an effective lidar ratio of the event and assess the performance of the algorithms by means of the root mean square error (RMSE) of the lidar- versus AERONET AOD time series. The Iterative algorithm exhibited the lowest deviation from the photometer at both 532 and 1064 nm (RMSE of 0.010 and 0.008, respectively), demonstrating the best performance. The Forward and Quasi-backscatter approaches followed closely, showing slightly higher deviations. In contrast, the Klett-Fernald algorithm showed the highest discrepancies at both 532 and 1064 nm (RMSE of 0.015 and 0.012, respectively). From the particle backscatter coefficients, the intensive properties backscatter-related Ångström exponent (BAE) at 532-1064 nm and the particle linear depolarization ratio (δ_p) at 532 nm can be derived, allowing effective classification of aerosols, clouds, and their mixing processes over time.

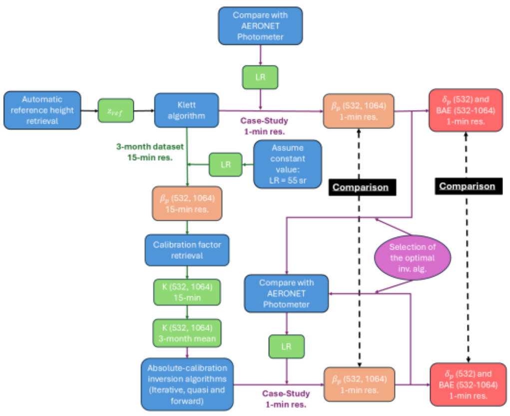

Figure 1. Flow chart of methodology

4. Results

The relative-calibration Klett-Fernald [3] and the absolute-calibration iterative algorithm [4] were applied to lidar measurements collected during a Saharan dust outbreak that occurred over Granada on 24–25 April 2025. This event exhibited a maximum AOD of approximately 0.5 at 532 nm. Around 01:00 UTC on 24 April, a Saharan dust layer arrived over Granada at an altitude of approximately 2 km agl. The dust intrusion persisted throughout 24 April (as confirmed by backward trajectories), resulting in a mixture of transported aerosols from Sahara with local aerosols from Granada, primarily associated with surface emissions.

The highest values of lidar signal were observed between 18:00 UTC on 24 April and 05:00 UTC on 25 April. Figure 2 presents a comparison between β_p retrieved from the Klett-Fernald and the iterative algorithm at 532 and 1064 nm, alongside the intensive properties (BAE 532–1064 nm and δ_p at 532 nm) during this period. The Klett-Fernald retrieval exhibits significant temporal variations in the backscatter coefficients, a phenomenon attributed to the instability of high-resolution reference height determination. These fluctuations hinder the clear characterization of the aerosol layers. In contrast, the iterative algorithm presents more robust inversions (with a temporal variance approximately three times lower for both λ), significantly enhancing the tracking of aerosol layer's evolution. Furthermore, the iterative algorithm converges to BAE values typical of literature, whereas the Klett-Fernald method tends to overestimate BAE due to the underestimation of β_p at 1064 nm. This absolute-calibration approach also enables the study of high-altitude aerosol layers and clouds, as it eliminates the requirement for a reference height in a clear-air region.

Focusing on the iterative algorithm time series with vertical resolution (*quicklooks*), a classification of the aerosol and cloud layers present during the event can be performed. The highest backscatter values in the aerosol layer occur around 2 km agl and are associated with coarse (BAE $\in [0.8,\ 0.9]$) and irregular ($\delta_p \approx 0.33$) particles, typical of Saharan dust. In contrast, the near-surface aerosol, between 0 and 2 km agl, exhibits lower backscatter, higher BAE (BAE ≈ 1.1) associated with finer particles, and low depolarization values ($\delta_p \in [0.10, 0.15]$), characteristic of continental/urban particles. Additionally, some points at 4 km agl around 17:00 UTC on 24 April and between 03:00 and 05:00 UTC on 25 April show very high backscatter attenuating the signal, associated with altocumulus clouds. Ångström exponent results are inconclusive due to noise, but the depolarization coefficient shows low values, consistent with water droplets. Between 6 and 11 km agl, elevated backscatter values are also observed with BAE < 0.5 and $\delta_p > 0.4$, linked to cirrus clouds (large ice crystals).

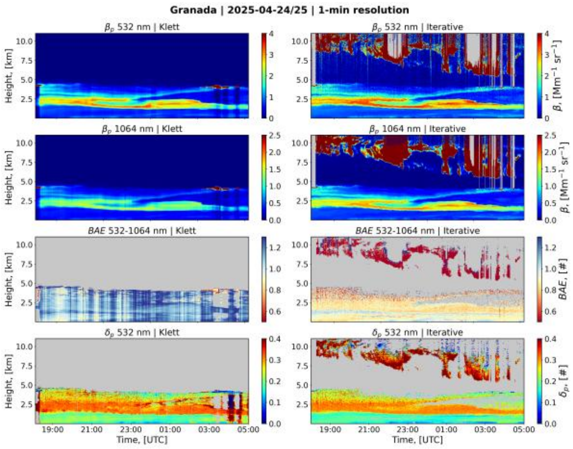

Figure 2. Time series with vertical resolution of particle backscatter coefficient at 532 and 1064 and the aerosol intensive properties: Ångström exponent at 532-1064 nm and linear particle depolarization at 532 nm retrieval with Klett-Fernald and iterative algorithms with 1-min temporal resolution between 18:00 and 5:00 UTC on April 24–25, 2025.

5. Conclusions

This study evaluated the performance of relative- (Klett-Fernald) and absolute-calibration (Iterative, Quasi-backscatter, and Forward) algorithms for retrieving aerosol optical properties at high spatiotemporal resolution (1 minute). The absolute-calibration inversion algorithms demonstrated better adaptability for tracking aerosol layers and clouds at high resolution, achieving better agreement with AERONET photometer values and showing less temporal variability. Among the three absolute-calibration algorithms considered, the iterative algorithm offers the best results, although the differences between them are less than 10% in this study case. The high-resolution iterative retrieval enabled a clear classification of atmospheric layers during the Saharan dust event. It successfully identified a mineral dust layer (around 2 km agl), continental/urban aerosols near the surface (0-2 km agl), and the presence of altocumulus and cirrus clouds at higher altitudes. In addition, since no reference height is required for signal inversion, aerosol optical properties can be studied for high-altitude aerosol layers and clouds or even aerosol layers below complete low-level cloud coverage.

6. References

[1] J. A. Bravo-Aranda *et al.*, "Study of mineral dust entrainment in the planetary boundary layer by lidar depolarisation technique," *Tellus B*, vol. 67, no. 1, Art. no. 26180, 2015.

[2] J. A. Benavent-Oltra *et al.*, "Overview of SLOPE I and II campaigns: Aerosol properties retrieved with lidar and sun–sky photometer measurements," *ACP*, pp. 1–33, 2021.

[3] J. D. Klett, "Stable analytical inversion solution for processing lidar returns," *App. Optics*, vol. 20, no. 2, pp. 211–220, 1981.

[4] P. Di Girolamo *et al.*, "Aerosol observations by lidar in the nocturnal boundary layer," *App. Optics*, vol. 38, no. 21, pp. 4585–4595, 1999.

[5] H. Baars *et al.*, "Target categorization of aerosol and clouds by continuous multiwavelength-polarization lidar measurements," *AMT,* vol. 10, no. 9, pp. 3175–3201, 2017.

[6] D. Li *et al.*, "Capabilities of an automatic lidar ceilometer to retrieve aerosol characteristics within the planetary boundary layer," *Rem. Sensing*, vol. 13, no. 18, p. 3626, 2021.

[7] P. Laj *et al.*, "Aerosol, clouds and trace gases research infrastructure (ACTRIS): The European research infrastructure supporting atmospheric science," *Bull. Amer. Meteor. Soc.*, vol. 105, no. 7, pp. E1098–E1136, 2024.

[8] H. Baars *et al.*, "An overview of the first decade of PollyNET: An emerging network of automated Raman-polarization lidars for continuous aerosol profiling," *ACP*, vol. 16, no. 8, pp. 5111–5137, 2016.

7. Acknowledgements

This work was supported by the Spanish Ministry of Science, Innovation and Universities through projects PID2023-151668OB-I00, PID2022-142708NA-I00, PID2023-151817OA-I00, PID2021-128008OB-I00, NATURAL (PID2024-158786NB-C21 and PID2024-158786NB-C22), ACTRIS-España (RED2024-153891-E); "European Union Next Generation EU/PRTR" and innovation program through project IRISCC (grant agreement No 101131261); Andalusian Regional Government through project DGP_PIDI_2024_01698; Horizon Europe program under the Marie Sklodowska-Curie Staff Exchange Actions with the projects GRASP-SYNERGY (grant agreement No 101131631) and AERIS (grant agreement No 101236396) and by University of Granada Plan Propio through Excellence Research Unit Earth Science and Singular Laboratory AGORA (LS2022-1) programs. S. Villalba-Torres and S. Fernández-Carvelo received funding from the Spanish Ministry of Research and Innovation (Agencia Estatal de Investigación), grant PREP2023-001538 and PRE2021-098351, respectively (co-funded by the European Social Fund Plus).